The paper was published in the proceedings of the 7th International Conference on Earthquake Geotechnical Engineering and was edited by Francesco Silvestri, Nicola Moraci and Susanna Antonielli. The conference was held in Rome, Italy, 17 – 20 June 2019.

Earthquake Geotechnical Engineering for Protection and Development of Environment and Constructions – Silvestri & Moraci (Eds)
 ISBN 978-0-367-14328-2

2D numerical modelling of seismic site effects in San Severino Marche

S. Renzi, J. Facciorusso & C. Madiai
Dipartimento di Ingegneria Civile e Ambientale, Università degli Studi di Firenze, Firenze, Italy

E. Gargini
Centro per la Protezione Civile, Università degli Studi di Firenze, Firenze, Italy

ABSTRACT: In the present paper, the results of 2D numerical analyses of seismic site effects at San Severino Marche (Macerata-Italy) are presented and discussed. The main purpose was to investigate the 2D effects due either to superficial or buried morphology, by comparing the results from two-dimensional analyses on two cross sections with those obtained in one-dimensional conditions. Site conditions, including morphological, stratigraphic and geotechnical subsoil characterization from geological-geotechnical survey are described in the first part of the paper. In the second part, the results of the 2D Local Seismic Response (LSR) analyses are given and commented. A large number of vertical soil profiles along the selected cross-sections were analyzed by means of 1D numerical modelling and different kind of amplification factors were computed with reference to peak ground accelerations and elastic response spectra to evaluate both topographic and basin-edge effects.

1 INTRODUCTION

The paper presents a case study of local seismic response analyses included in a project, sponsored and funded by the Italian Government Commissioner for the Reconstruction (Ord. 24/ 2017), involving the 138 municipalities most affected by the 2016-2017 Central Italy seismic sequence. The project was aimed at achieving a third level of seismic microzoning as defined in the Italian standards for Seismic Microzonation (Working Group SM, 2008) and provided for performing 1D and 2D numerical simulation of seismic ground response.

The case study presented here was selected with the main purpose of evaluating the 2D effects due either to superficial or buried morphology.

Since the 70s, many researchers have been investigated the 2D basin effects due to buried morphology by means of analytical, numerical, experimental or combined approaches. More recently, some Authors have also considered how to introduce in seismic building codes an appropriate Aggravation Factor (AF), defined as the ratio between 2D and 1D acceleration spectra at the basin surface, to account for the basin effects in seismic ground response (Chávez-García & Faccioli 2000, Pitilakis et al. 2015, Madiai et al. 2015, 2017).

On the other hand, topographic effects are the subject of many studies (Geli et al 1988, Assimaki et al, 2005, Ashford et al 1997, Paolucci 2002, among others) which point out their frequency dependence. In a simplified way, they are taken into account in several international Seismic codes (European Code EC8, Italian Code NTC 2018, French Code AFPS 1995).

The studied area is located in the municipality of San Severino Marche which is a town lying in proximity to the eastern part of the Umbro-Marchigiano Apennines, 50km far from the Adriatic see. It was struck by the 2016-2017 Central Italy seismic sequence and suffered significant damages in several suburban areas, i.e. Uvaiolo, Settempeda and Mazzini neighborhoods, where severe damages were mainly observed in buildings dating back to 70s and 80s, for some of which complete demolition was necessary.

The third level seismic microzonation of San Severino Marche was focused in both the urban areas (the old town with a rich historical heritage) as well as in the suburban neighborhood, covering an area lying between 225 and 342m above sea level.

Accurate 2D-seismic response analyses were performed along two different cross-sections with a length respectively of about 3115 and 2250m. LSR2D, a finite element software (STACEC, 2017), was used for the analyses. Moreover, 1D ground response analyses were performed by means of STRATA computer program (Rathje and Kottke, 2013) on a number of vertical profiles located along the two analyzed cross-sections.

2 GEOLOGICAL AND GEOTECHNICAL FEATURES OF THE SECTIONS

The detailed geological subsoil model, the geometry and the geotechnical properties of the bedrock and the covering deposits, along the two analyzed AA' and BB' cross-sections (Figure 1), were inferred from existing data integrated with geophysical investigation and geotechnical in situ and laboratory tests carried out as part of the activities leading up to Seismic Microzonation of level III in the Macroarea – Marche 1 (Presidenza del Consiglio dei Ministri - OCDPC n. 394/2016).

The analyzed cross-sections are characterized by covering soils with different geological depositional environment: eluvial-colluvial, alluvial, slope debris and fluvial terraces.

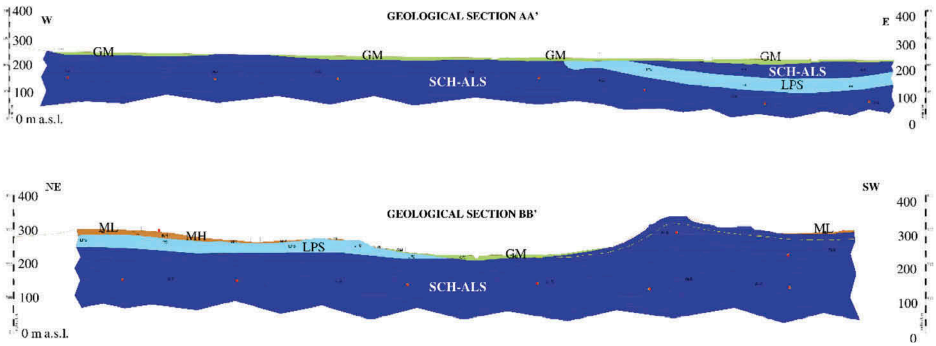

Figure 1. Sketch of the analysed cross-sections AA′ and BB′.

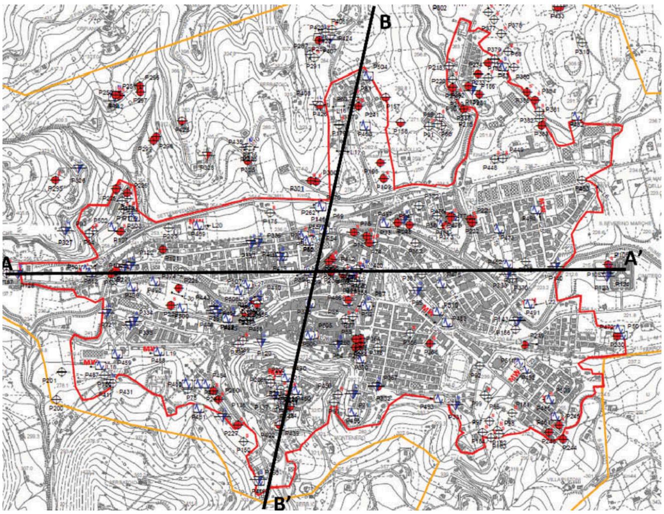

Figure 2. Analysed cross-sections.

Two different geologic and seismic bedrock was identified in the area, namely Schlier Unit (SCH/ALS) that consists mainly of limestones, calcareous limestones and gray clayey limestones and Gessoso-Solfifera Unit (GES/LPS), consisting mainly of gypsum and rock salt layers. This latter, which lies over the SCH/ALS Unit at the east side of A-A' section and at the north side of B-B' section, shows thicknesses of few tens of meters along the B-B' section that reach up to 100m along the A-A' section.

Figure 2 shows the large amount of geophysical and geotechnical data used to define the subsoil model with the location of the investigations carried out within the MS3 project, namely two boreholes (S1 and S2) equipped for Down-Hole tests, performed by the Department of Civil and Environmental Engineering (DICeA), University of Florence. Two undisturbed soil samples were collected from S1 borehole and tested in laboratory to determine physical parameters and non-linear dynamic shear stress–strain behaviour of the covering fine-grained materials.

The main characteristics of the two tested samples are summarized in Table 1.

Figure 3 shows the RC experimental data and the best fitting curves of the normalized shear modulus and damping ratio versus shear strain for the fine grained covering soil material. The Yokota et al. (1981) model, expressed by the following equations, was adopted to fit the experimental data for the $G(\gamma)/G_0$ and $D(\gamma)$ curves.

Table 1. Main characteristics of the tested samples from MH-ML lithological Unit.

site	CI	USCS classification	z [m]	γ [kN/m^3]	w_L [%]	PI [%]	σ'_c [kPa]
Uvaiolo	S1C1	CL	6.5÷7.1	19.46	35	19	130
	S1C2	CL	15.0÷15.5	19.81	36	18	120

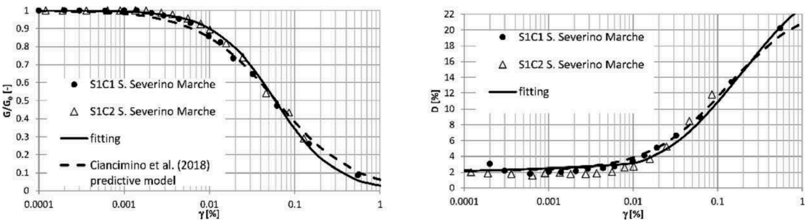

Figure 3. Normalized shear modulus (a) and damping ratio (b) versus shear strain.

$$\frac{G}{G_0} = \frac{1}{1 + \alpha \cdot \gamma^{\beta}} \tag{1}$$

$$D = D_{\max} \cdot e^{\lambda \frac{G}{G_0}} \tag{2}$$

In equation 1 and 2, D_{max} is the maximum damping ratio; α, β and λ are the soil fitting parameters (α = 32.961, β = 1.236, λ = 2.667 and D_{max} = 31.658).

Figure 3 also shows a very good agreement between the Yokota curves, $G(\gamma)/G_0$ and $D(\gamma)$, fitting the experimental data and the corresponding curves from the predictive model proposed by Ciancimino et al. 2018 (submitted) for fine-grained materials of Central Italy, evaluated for plasticity index PI=18.5% and effective mean confining pressure σ'_c=125 kPa (average values of the two tested samples).

3 SEISMIC INPUT MOTION

The seismic input motion assumed to perform the numerical analyses was a set of seven actual signals with an average response spectrum matching the site reference spectrum provided by

Table 2. Characteristics of the spectrum compatible set of accelerograms.

input	input code	station name	date	PGA [m/s^2]	M_W
I1	3A.MZ11..HNE.D.20161030.064018	Bedrock nord Sant'Angelo	30/10/2016	0.17	6.1
I2	3A.MZ19..HNN.D.20161030.064018	Pasciano cimitero	30/10/2016	0.39	6.1
I3	IT.CLO..HGE.D.20161026.191806	Castelluccio di Norcia	26/10/2016	0.18	5.9
I4	IT.CLO..HGN.D.20161026.191806	Castelluccio di Norcia	26/10/2016	0.19	5.9
I5	IT.MM0..HGE.D.20161030.064018	Montemonaco	30/10/2016	0.19	6.5
I6	IT.MMO..HGN.D.20161030.064018	Montemonaco	30/10/2016	0.19	6.5
I7	IV.T1212..HNE.D.20161026.171036	Avendita (PG)	26/10/2016	0.18	5.4

NTC18 for a return period of 475 years. The extraction of the spectrum compatible set has been done using the software RexeLite, without applying any scale factor (Working Group Seismic Input, 2017).

The main characteristics of the selected accelerograms are synthetized in Table 2.

4 NUMERICAL ANALYSES AND RESULTS

The 2D ground response analyses were performed by means of the software LSR2D (STACEC, 2017), a time domain, equivalent linear, computer program that implements the Finite Element Method. Analyses are performed in total stress for elastic bedrock conditions.

The analysis domain was subdivided in triangular elements to better define morphological and topographic irregularities and boundaries. To allow the transfer of the highest frequency fmax of the input motion considered as significant (20Hz), the maximum dimension Δh of the triangular finite elements within each soil layer was assumed according to the well-known relation suggested by Kuhlemeyer and Lysmer (1973)

The seismic input motion (vertically incident SV shear waves and P compression waves) are applied simultaneously to all the nodes at the base boundary of the analysis domain and the equation system is solved in the time domain using the CAA method (Constant Average Acceleration Method). Free-field conditions are realized at the lateral boundaries by means of normal and tangential viscous dampers connecting the lateral boundary nodes of the analysis domain to as many nodes of appropriate free-field soil columns (Figure 4).

The 1D numerical analyses were performed by means of STRATA computer program (Rathje and Kottke, 2013) that implements a total stress, frequency domain, equivalent linear model. The maximum height for each layer was assumed according to the previously mentioned Kuhlemeyer and Lysmer (1973) criterion.

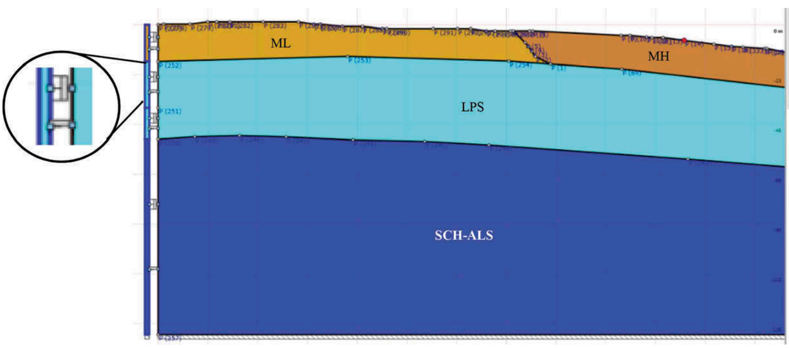

Figure 4. Free-field conditions at the lateral boundaries (normal and tangential viscous dampers).

Table 3. Main physical and mechanical soil properties.

Material	ρ [kg/m^3]	V_S [m/s]	ν [-]	D_0 [%]	Stiffness decay and Damping curve
GM	1975	365	0.30		Rollins et al. (1989)
MH	1963	268	0.38		L2
ML	1963	268	0.38		L2
SCH/ALS	2250	950	0.30	0.5	$G(\gamma)/G_0 = 1$, $D(\gamma) = 0.5\%$
GES/LPS	2050	550	0.30	0.5	$G(\gamma)/G_0 = 1$, $D(\gamma) = 0.5\%$

For the purpose of seismic ground response numerical modelling, each lithological unit was characterized by means of: density (ρ), shear waves velocity (V_S), Poisson ratio (ν) and curves of damping ratio (D) and normalized shear modulus with respect to initial modulus (G/G_0) with shear strain (γ). The main physical and mechanical soil properties of each unit assumed for the numerical analyses are summarized in Table 3.

V_S profiles for each lithological Unit was derived from the results of Down Hole and MASW (Multichannel Analysis of Surface Waves) tests, combined with experimental HVSR (Horizontal to Vertical Spectral Ratio) measurements.

The shear modulus and damping ratio curves for the L2 (MH-ML) lithological Unit were obtained from Resonant Column (RC) tests performed by the Geotechnical Laboratory of the University of Florence on two soil samples taken from S1 borehole carried out at the site located in Uvaiolo neighborhood in the municipality of San Severino Marche, where the Unit was encountered.

The curves $G(\gamma)/G_0$ and $D(\gamma)$ proposed by Rollins et al. (1989) were assumed for GM lithological Unit.

Since the results obtained on A-A' section are not significant for the purposes of the present study, only the results concerning the B-B' section area presented and discussed in the following.

Results in terms of Aggravation Factor (AF) are reported in Figure 5. Numerical values of a set of selected point showing higher values of AF are reported in Table 4. Period range of interest was discretized in classes of width 0.1s.

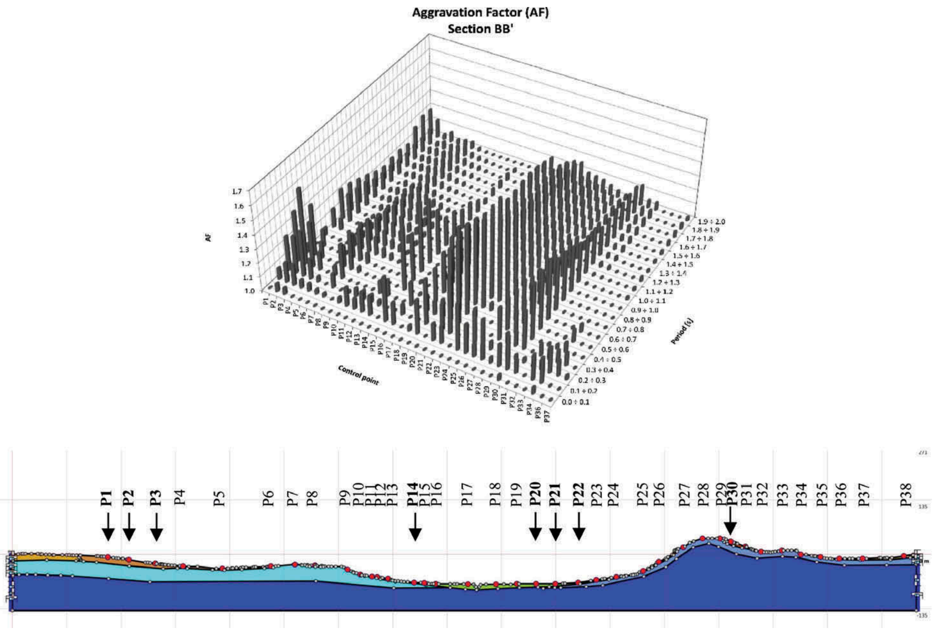

Figure 5. Aggravation Factor (Section BB').

Table 4. Aggravation Factor (Section BB') – numerical values.

T [s]	0.0 ÷ 0.1	0.1 ÷ 0.2	0.2 ÷ 0.3	0.3 ÷ 0.4	0.4 ÷ 0.5	0.5 ÷ 0.6	0.6 ÷ 0.7	0.7 ÷ 0.8	0.8 ÷ 0.9	0.9 ÷ 1.0	1.0 ÷ 1.1	1.1 ÷ 1.2	1.2 ÷ 1.3	1.3 ÷ 1.4	1.4 ÷ 1.5	1.5 ÷ 1.6	1.6 ÷ 1.7	1.7 ÷ 1.8	1.8 ÷ 1.9	1.9 ÷ 2.0
P1	-	1.08	1.24	1.36	1.06	-	1.05	1.13	1.21	1.20	1.17	1.14	1.11	1.09	1.10	1.10	1.09	1.16	1.19	1.18
P2	1.05	1.14	1.26	1.54	1.36	1.12	-	1.08	1.20	1.18	1.17	1.13	1.12	1.12	1.10	1.10	1.10	1.10	1.11	1.12
P3	1.04	1.15	1.32	1.32	1.12	-	-	-	-	-	-	1.02	1.02	-	1.02	1.03	1.03	1.04	1.03	1.03
P14	-	-	-	-	1.45	1.33	1.49	1.44	1.31	1.20	1.18	1.13	1.12	1.07	1.03	1.05	1.05	1.04	1.02	1.00
P20	-	-	-	1.12	1.35	1.36	1.39	1.33	1.32	1.29	1.26	1.24	1.24	1.18	1.18	1.19	1.18	1.18	1.16	1.12
P21	-	1.11	1.18	1.50	1.58	1.54	1.52	1.43	1.40	1.35	1.32	1.29	1.28	1.21	1.21	1.22	1.21	1.21	1.19	1.15
P22	-	1.12	1.42	1.58	1.62	1.56	1.53	1.45	1.41	1.36	1.32	1.29	1.29	1.22	1.22	1.23	1.21	1.21	1.20	1.16
P30	1.03	1.23	1.02	1.26	1.39	1.41	1.42	1.36	1.34	1.31	1.27	1.26	1.25	1.20	1.20	1.20	1.19	1.19	1.19	1.14

5 DISCUSSION AND CONCLUSIONS

The maximum Aggravation Factors of the whole section are found to lay in the range 0.2÷0.9s, with values ranging between 1.31 and 1.62 and an average value of 1.46. They are particularly concentrated in the range 0.3÷0.7s, showing an average value of 1.51.

In particular points P1, P2 and P3 located in the North-East side of the section shows the maxima Aggravation Factors in a very limited range of period, i.e. 0.2÷0.4s with values ranging between 1.24 and 1.54. Points located in the area near the edges of the valley, i.e. P14, P20, P21 and P22, show higher Aggravation Factor in the range 0.4÷0.9s, with values ranging between 1.31 and 1.62. Also Point P30, located at the top of the hill in the South-West side shows higher Aggravation Factors in the same range of period.

For points P1, P2, P3 and P30 the topographic amplification effect is self-evident. For points P14, P20, P21 and P22 the basin edge effect is evidenced.

In this study, the 2D effects due either to superficial or buried morphology, was investigated by comparing the results from two-dimensional analyses on two cross sections with those obtained in one-dimensional conditions. In order to determine the difference between the results of one and two dimensional dynamic analyses, the acceleration spectra which were calculated for different points of the sections by using 2D dynamic analyses were divided by the ones calculated with 1D dynamic analyses, so that the Aggravation Factors were obtained.

Results of this study are expected to be useful for estimating the effect of second dimension on the spectral acceleration values obtained for basin edge sections from 1D dynamic analyses.

ACKNOWLEDGMENTS

The authors would like to thank drs. Alessandro Onorati, Marcello Maccari, Giorgio Cipolletti, Francesco Bassano, Francesco Carboni for providing the geological cross-sections.

This study was partially supported by Dipartimento della Protezione Civile Nazionale-Rete dei Laboratori Universitari di Ingegneria Sismica (DPC-ReLUIS) funds.

REFERENCES

AFPS 1994. Recommandation AFPS 90 pour la rèdaction de règles relatives aux ouvrages et installations à réaliser dans les régions sujettes aux seismes. Presses de l'Ecole Nationale des Ponts et Chaussée, 1994

Ashford S.A., Sitar N., Lysmer J., Deng N. 1997 Topographic effects on the seismic response of steep slopes. *Bull Seismol Soc Am 7(3):701–709*

Assimaki D., Gazetas G., Kausel E. 2005. Effects of local soil conditions on the topographic aggravation of seismic motion: parametric investigation and recorded field evidence from the 1999 Athens earthquake. *Bull Seismol Soc Am 95(3):1059–1089*

Chávez-García F. J. & Faccioli E. 2000. Complex site effects and building codes: Making the leap, *J. Seismol. 4:23–40*.

Ciancimino A., Lanzo G., Alleanza G. A., Amoroso S., Bardotti R., Biondi G., Cascone E., Castelli F., Giulio A. D., D'onofrio A., Foti S., Lentini V., Madiai C., Vessia G. 2018 (submitted). Dynamic characterization of fine-grained soils in Central Italy by laboratory testing. *Bulletin of Earthquake Engineering*.

Eurocode 8 2004. Design of structures for earthquake resistance, Part 1: General rules, seismic actions and rules for buildings, EN 1998–1:2004, European Committee for Standardization (CEN), Brussels, Belgium.

Geli L, Bard PY, Jullen B. 1988. The effect of topography on earthquake ground motion: a review and new results. *Bull Seismol Soc Am 78:42–63*

Italian Government Commissioner for the Reconstruction 2017. Ordinanza n. 24 del 12 maggio 2017.

Kuhlemeyer R.L., Lysmer J. 1973. Finite element method accuracy for wave propagation problems. *J. Soil Mech. Found. Eng. Div. ASCE 99 (SM5):421–427*

Madiai C., Facciorusso J., Gargini E., Vannucchi, G., Baglione M. 2015. A methodology for advanced seismic microzoning using 2D analyses: the case study of Barberino di Mugello, Florence, Italy, In: *Engineering Geology for Society and Territory. vol. 5, p. 1081–1084*, Springer, ISBN: 9783319090474, Torino (Italy), 15–19 September 2014, doi: 10.1007/978-3-319-09048-1_205

Madiai C., Facciorusso J., Gargini E. 2017. Numerical Modeling of Seismic Site Effects in a Shallow Alluvial Basin of the Northern Apennines (Italy), *Bulletin of the Seismological Society of America, vol. 107, No. 5, pp. 2094–2105*, October 2017, DOI 10.1785/0120160293

NTC 2018. Norme Tecniche per le Costruzioni. Decreto Ministero Infrastrutture. GU Serie Generale n.42 del 20-02-2018 - Suppl. Ordinario n. 8, Istituto Poligrafico e Zecca dello Stato, Roma(www.cslp.it).

Paolucci R. 2002, Amplification of earthquake ground motion by steep topographic irregularities. *Earthquake Engng Struct. Dyn. 2002; 31:1831–1853* (DOI: 10.1002/eqe.192)

Pitilakis K., Riga E., Anastasiadis A., Makra K. 2015. New elastic spectra, site amplification factors and aggravation factors for complex subsurface geometry towards the improvement of EC8, 6th International Conference on Earthquake Geotechnical Engineering, Christchurch, New Zealand, 1–4 November 2015.

Presidenza del Consiglio dei Ministri - OCDPC n. 394 2016. Ulteriori interventi urgenti di protezione civile conseguenti all'eccezionale evento sismico che ha colpito il territorio delle Regioni Lazio, Marche, Umbria e Abruzzo il 24 agosto 2016.

Rathje E.M., Kottke A. 2013. Strata. http://nees.org/resources/strata

Rollins K.M., Evans M.D., Diehl N.B., Daily W.D. 1998. Shear modulus and damping relationships for gravels, *Journal of Geotechnical and Geoenvironmental Engineering, Vol.124, Issue 5, pp.396–405*, ASCE (American Society of Civil Engineers), New York, NY.

STACEC srl 2017. LSR2D - Risposta sismica locale. www.stacec.it

Working Group SM 2008. Guidelines for Seismic Microzonation, Conference of Regions and Autonomous Provinces of Italy – Civil Protection Department, Rome. (italian version: Gruppo di Lavoro MS, Indirizzi e criteri per la microzonazione sismica. Conferenza delle Regioni e delle Province Autonome - Dipartimento della Protezione Civile.

Working Group Seismic Input 2017. P4.5 Definizione dell'input sismico da utilizzare per le analisi numeriche di risposta sismica locale 1D e 2D, pp.1–154 (in italian). Technical Report, Prot. CNR IGAG n. 0002738 del 09/08/2017

Yokota K., Imai T., Konno M. 1981. Dynamic deformation characteristics of soils determined by laboratory tests, OYOTech. Rept. 3:13–37.